Oxomolybdenum(V)/Iron(III) Porphyrinate Complexes: Effect of Axial Ligand Plane Orientation on Complex Stability, Reduction Potential, and NMR and EPR Spectra

Partha Basu, Arnold M. Raitsimring, John H. Enemark,* and F. Ann Walker*

Department of Chemistry, University of Arizona, Tucson, Arizona 85721

Received August 2, 1996[⊗]

The compounds {5,10,15-tri-*p*-tolyl-20-[[2,3-[((hydrotris(3,5-dimethylpyrazolyl)borato)oxomolybdenio)dioxy]-phenyl]porphyrinato}bis(2-methylimidazole)iron(III) chloride, Fe(2,3-Mo-TTP)(2MeImH)$_2$Cl (**1**), and {5,10,15-tri-*p*-tolyl-20-[3,4-[((hydrotris(3,5-dimethylpyrazolyl)borato)oxomolybdenio)dioxy]phenyl]porphyrinato}bis(2-methylimidazole)iron-(III) chloride, Fe(3,4-Mo-TTP)(2MeImH)$_2$Cl) (**2**), have been prepared in order to assess the effect of axial ligand plane orientation upon the stability, reduction potential, and NMR and EPR spectra of these novel (porphryinato)-iron(III)−Mo(V) systems that possess two $S = {}^1/_2$ metal centers. The proton NMR spectra of **1** and **2** are characteristic of perpendicular orientation of the planes of the axial 2MeImH ligands. These results contrast with those previously reported (Basu, P.; Shokirev, N. V.; Enemark, J. H.; Walker, F. A. *J. Am. Chem. Soc.* **1995**, *117,* 9042−9055) for the analogous compounds with NMeIm as the axial base (**3**, **4**) whose ^{1}H NMR spectra are characteristic of one or both axial ligands in parallel planes. The equilibrium constants (β_2) for binding the bulky 2MeImH ligands of **1** and **2** are more than an order of magnitude smaller than those for NMeIm binding to **3** and **4**. Three distinct pseudo-Nernstian one-electron couples are observed for **1** and **2** in DMF that can be assigned to the Fe(III/II), Mo(V/IV), and Fe(II/I) reductions, with the Fe(III/II) couple being most positive. The Fe(III/II) and Mo(V/IV) potentials are similar to those for **3** and **4** and only slightly perturbed from those of the individual isolated components. The EPR spectrum of **1** shows features due to Mo(V) and low-spin Fe(III) that are perturbed by weak exchange coupling (2.6 GHz, 0.078 cm^{-1}) between the two metal centers which are separated by ∼7.9 Å. The "large g_{max}" feature characteristic of the 2MeImH adducts of Fe(III) tetraphenylporphyrinates is shifted toward the Mo(V) signal to 2.85; the anisotropy of the Mo(V) signal is lost, and no molybdenum hyperfine can be detected. The EPR spectrum of **2**, which has a metal−metal separation of ∼9.4 Å, shows an unperturbed "large g_{max}" value of 3.41 for the Fe(III) center. The Mo(V) part of the spectrum is slightly perturbed from that of the precursor catecholate complex but is essentially identical to that of **4**, which exhibits a rhombic Fe(III) signal.

Introduction

A majority of the *b*-type cytochromes contain at least one histidine axial ligand coordinated to the iron center. The other axial ligand is either histidine or methionine. In proteins, the orientations of the imidazole rings of the histidines are fixed by the heme pocket and by the hydrogen bonds to the histidinyl nitrogen (N−H). A planar imidazole ligand can be aligned at any angle relative to the vector connecting an opposing pair of pyrrole nitrogens of the porphyrin ring. In the case of bis(histidine)-ligated centers, the planes of the two axial ligands can be parallel or perpendicular to each other or they can be oriented at any intermediate angle to one other. In addition, the axial ligands can be tilted so that the Fe−N (axial) vector is not normal to the porphyrin plane. These conformational diversities lead to a wide variation in molecular properties. However, it has often been very difficult to study the effect of these factors on the observed properties of proteins because other factors such as molecular size, hydrophobicity, surface charge, and ionic strength also affect the properties of proteins, and it is difficult to quantitate the effect of each.

For several years we have been investigating model compounds designed to explore how the relative orientations of the imidazole rings affect the properties of the heme center and its interaction with other prosthetic group(s).[1−3] For low-spin Fe(III) porphyrinate complexes, as with *b*-type cytochromes, the 3e(π) orbitals of the porphyrin ring and the dπ orbitals of the metal can overlap to form two low-energy molecular orbitals that are mainly porphyrin in character.[4,5] Two high-energy (valence) molecular orbitals are also formed that are mainly metal in character and which contain three electrons. Both unsymmetrical substitution in the porphyrinato ring and a coordinated histidine that is prevented from rotation (as in the heme pocket) can break the degeneracy. In *parallel axial ligand plane orientation*, the coordinated-nitrogen p$_\pi$ orbitals of both of the axial histidines interact with the same d$_\pi$ orbital of the low-spin iron(III),[6] shifting that orbital to higher energy and thus causing it to be preferentially occupied by the odd electron. However, when the axial ligands are in mutually *perpendicular orientation*, each d$_\pi$ orbital will interact with a nitrogen p$_\pi$ orbital from an axial ligand (Figure 1). Thus, in parallel orientation one d$_\pi$ orbital will be preferentially destabilized, while in

[⊗] Abstract published in *Advance ACS Abstracts,* February 15, 1997.

(1) Walker, F. A.; Simonis, U. Proton NMR Spectroscopy in Model Hemes. In *NMR of Paramagnetic Molecules*; Biological Magnetic Resonance, Vol. 12; Berlinger, L. J., Reuben, J., Eds.; Plenum Press: New York, 1993; pp 133−274 and references cited therein.

(2) Walker, F. A.; Simonis, U. In *Encyclopedia of Inorganic Chemistry*; King, R. B., Ed.; Wiley & Sons: Chichester, U.K., 1994; Vol. 4, pp *4*, 1785−1846 and references cited therein.

(3) Basu, P.; Raitsimring, A. M.; LaBarre, M. J.; Dhawan, I. K.; Weibrecht, J. L.; Enemark, J. H. *J. Am. Chem. Soc.* **1994**, *116*, 7166−7176.

(4) Longuet-Higgins, H. C.; Rector, C. W.; Platt, R. R. *J. Chem. Phys.* **1950**, *18*, 1174−1181.

(5) (a) Greenwood, H. H. *Computing Methods in Quantum Organic Chemistry*; Wiley-Interscience: New York, 1972. (b) Stretwieser, A., Jr. *Molecular Orbital Theory for Organic Chemists*; John Wiley: New York, 1961.

(6) Walker, F. A.; Simonis, U.; Zhang, H.; Walker, J. M.; Ruscitti, T. M.; Kipp, C.; Amputch, M. A.; Castillo, B. V.; Cody, S. H.; Wilson, D. L.; Graul, R. E.; Yong, G. J.; Tobin, K.; West, J. T.; Barichievich, B. A. *New J. Chem.* **1992**, *16*, 609−620.

S0020-1669(96)00945-7 CCC: $14.00

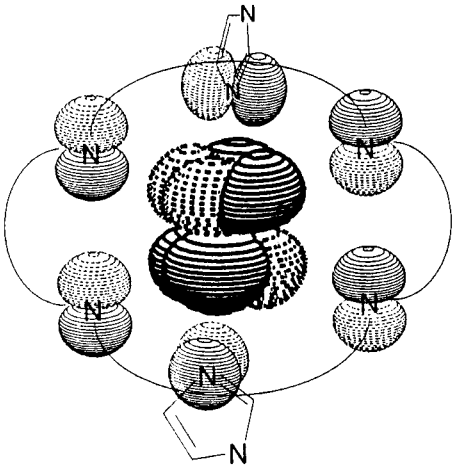

Figure 1. Interaction of the axial ligand planes and porphyrin nitrogens with the metal dπ orbitals. The involved orbitals are metal d_{xz}, and d_{yz}, porphyrin nitrogen pπ, and axial ligand nitrogen pπ. Note that, due to the perpendicular orientation of the axial ligand planes, the two axial ligands interact with two different metal dπ orbitals.

perpendicular orientation both d_π orbitals will be destabilized to the same extent. Clear evidence of this difference in electronic structure has observed in the Mössbauer and EPR spectra of model hemes recorded at low temperatures.[7,8] Spin delocalization of the odd electron into the higher energy orbital of the porphyrinate ring also results in the distinctive contact shift patterns observed in the NMR spectra of the pyrrole substituents.[1] When the ligands are in the parallel orientation, nondegeneracy in the d_π orbitals leads to large differences in spin density at different pyrrole positions and, therefore, a large spread in the pyrrole proton shifts is observed.[9,10] The small energy separation of the d_π orbitals for perpendicular orientation is expected to lead to similar spin density at the different pyrrole positions and a smaller spread of the pyrrole proton resonances. Axial ligands such as *N*-methylimidazole (NMeIm) adopt parallel orientation, whereas the sterically bulky 2-methylimidazole (2MeImH) adopts perpendicular orientation, both in the solid state[11,12] and in solution.[13,14] Since an electron is added upon reduction of iron(III) to iron(II) and that electron goes into the higher energy e(π) orbital, a change in the relative energy caused by ligand plane orientation may also affect the reduction potential.[8]

An unsymmetrically substituted porphyrinate ring can break the symmetry of the valence e(π) orbitals, creating a separation in energy, ΔE_π.[15] This energy separation can be modulated by the electron-withdrawing/donating ability of the substituents but usually is much smaller in magnitude than that created by a planar axial ligand at a fixed orientation or two planar axial ligands in parallel orientation.[10] We have shown that a *meso* position carrying a strong electron-donating or -withdrawing substituent relative to the others can cause significant change in the spin-density distribution.[1,15] The molecules of the present study have a small substituent effect and thus are well suited for determining the effects of ligand plane orientation on the observed properties, e.g., NMR and EPR spectra. Here we demonstrate that suitably designed molecules can show the dramatic effect of the ligand plane orientation on the properties of the Fe(III) porphyrinate center.

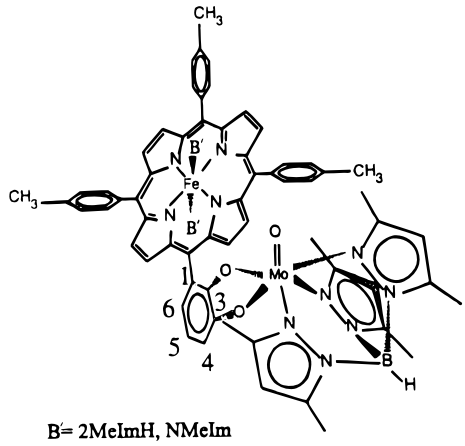

Figure 2. Structure of {5,10,15-tri-*p*-tolyl-20-[2,3-[((hydrotris(3,5-dimethylpyrazolyl)borato)oxomolybdenio)dioxy]phenyl]porphyrinato}-bis(2-methylimidazole)iron(III) chloride, Fe(2,3-Mo-TTP)(B′)$_2$Cl (**1** and **3**).

Heme is one of the most prevalent prosthetic groups, and it often coexists with one or more other prosthetic groups. One such example is sulfite oxidase, a heme-containing molybdoprotein that is essential for sulfur metabolism in animals.[16] It is believed that the oxidation of sulfite to sulfate occurs at the molybdenum center during an oxygen atom transfer reaction. The two-electron-reduced molybdenum center is then oxidized intramolecularly by its prosthetic heme partner in two one-electron steps.[17,18] Consequently, in the catalytic process, molybdenum passes through three different oxidation states, Mo(VI), Mo(V), and Mo(IV). Of these, only Mo(V) is paramagnetic (d^1) and detectable by EPR spectroscopy. We are interested in understanding the interaction of the paramagnetic molybdenum(V) center with its partner prosthetic group, the heme center. As a part of our program to understand the interprosthetic group interaction in SO, we recently prepared {5,10,15-tri-*p*-tolyl-20-[2,3-[((hydrotris(3,5-dimethylpyrazolyl)borato)oxomolybdenio)dioxy]phenyl]porphyrinato}bis(*N*-methylimidazole)iron(III) chloride, [Fe(2,3-Mo-TTP)(NMeIm)$_2$]Cl) (**3**) (Figure 2) and {5,10,15-tri-*p*-tolyl-20-[3,4-[((hydrotris(3,5-dimethylpyrazolyl)borato)oxomolybdenio)dioxy]phenyl]-porphyrinato}bis(*N*-methylimidazole)iron(III) chloride, [Fe(3,4-Mo-TTP)(NMeIm)$_2$]Cl (**4**), as first-generation models. We have reported the electronic spin−spin coupling between the iron(III) center ($S = {}^1/_2$) and the oxomolybdenum(V) center ($S = {}^1/_2$) observed at low temperatures by EPR spectroscopy.[3] Molecular modeling data for [Fe(2,3-Mo-TTP)(NMeIm)$_2$]Cl showed that in this system the two metal centers are separated by ∼7.9 Å. From EPR measurements at low temperatures, we

(7) (a) Safo, M. K.; Gupta, G. P.; Walker, F. A.; Scheidt, W. R. *J. Am. Chem. Soc.* **1991**, *113*, 5497−5510. (b) Safo, M. K.; Gupta, G. P.; Watson, C. T.; Simonis, U.; Walker, F. A.; Scheidt, W. R. *J. Am. Chem. Soc.* **1992**, *114*, 7066−7075.
(8) Walker, F. A.; Huynh, B. H.; Scheidt, W. R.; Osvath, S. R. *J. Am. Chem. Soc.* **1986**, *108*, 5288−5297.
(9) Basu, P.; Shokhirev, N. V.; Enemark, J. H.; Walker, F. A. *J. Am. Chem. Soc.* **1995**, *117*, 9042−9055.
(10) Shokhirev, N. V.; Walker, F. A. *J. Phys. Chem.* **1995**, *99*, 17795−17804.
(11) Scheidt, W. R.; Kirner, J. F.; Hoard, J. L.; Reed, C. A. *J. Am. Chem. Soc.* **1987**, *109*, 1963.
(12) Munro, O. Q.; Marques, H. M.; Debrunner, P. G.; Mohanrao, K.; Scheidt, W. R. *J. Am. Chem. Soc.* **1995**, *117*, 935−954.
(13) Walker, F. A.; Simonis, U. *J. Am. Chem. Soc.* **1991**, *113*, 8652−8657.
(14) Nakamura, M.; Tajima, K.; Tada, K.; Ishizu, K.; Nakamura, N. *Inorg. Chim. Acta* **1994**, *224*, 113 −124.
(15) Tan, H.; Simonis, U.; Shokhirev, N. V.; Walker, F. A. *J. Am. Chem. Soc.* **1994**, *116*, 5784−5790.
(16) Rajagopalan, K. V. In *Advances in Enzymology and Related Areas of Molecular Biology*; Meister, A., Ed.; John Wiley: New York, 1991; Vol. 64, pp 215−290.
(17) (a) Neame, P. J.; Barber, M. J. *J. Biol. Chem.* **1989**, *264*, 20894−20901. (b) Cohen, H. J.; Fridovich, I. *J. Biol. Chem.* **1971**, *246*, 359−366, 367−373.
(18) Enemark, J. H.; Young, C. G. *Adv. Inorg. Chem.* **1993**, *40*, 1−88.

concluded that the spin−spin coupling is primarily exchange in nature.[3,19] However, in the isomeric [Fe(3,4-Mo-TTP)(NMeIm)$_2$]Cl the two centers are ∼9.4 Å apart, and the spin−spin coupling is dominated by the dipolar interaction.[3,19] From a detailed NMR investigation, we showed that in [Fe(2,3-Mo-TTP)(NMeIm)$_2$]Cl one NMeIm is prevented from rotating, even at room temperature, and the other NMeIm is either aligned parallel to the first one or is rotating rapidly.[9] We also found that the molybdenyl substituent had little electronic effect on the porphyrin. Thus, this system is well suited for studying the effects of ligand plane orientation on the observed properties such as the spin−spin coupling between the two metal centers. To examine the effect of the ligand plane orientation on the weak spin−spin coupling, we prepared {5,10,15-tri-*p*-tolyl-20-[2,3-[((hydrotris(3,5-dimethylpyrazolyl)borato)oxomolybdenio)-dioxy]phenyl]porphyrinato}bis(2-methylimidazole)iron(III) chloride, Fe(2,3-Mo-TTP)(2MeImH)$_2$Cl (**1**), and {5,10,15-tri-*p*-tolyl-20-[3,4-[((hydrotris(3,5-dimethylpyrazolyl)borato)oxomolybdenio)dioxy]phenyl]porphyrinato}bis(2-methylimidazole)iron-(III) chloride, Fe(3,4-Mo-TTP)(2MeImH)$_2$Cl (**2**). Here we report their electrochemistry and their electronic, NMR, and EPR spectral properties.

Experimental Section

Materials. All solvents for syntheses were purchased either from Aldrich or from Fisher and were distilled before use. NMR solvents (99.5% deuterated) were purchased from either Aldrich or Cambridge Isotopes and were dried over 4 Å molecular sieves.

Physical Measurements. Infrared spectra were recorded on a Perkin-Elmer 983 spectrophotometer with samples as KBr pellets, unless otherwise specified. Cyclic voltammetry was performed on dimethylformamide solutions using a BAS CV 50W system with a three-electrode configuration. The reference electrode was a silver/silver chloride electrode (Ag/AgCl), a BAS Model MF 2012 graphite electrode was used as the working electrode, and a platinum wire served as the counter electrode. The sample concentrations were ∼1 mM with a large excess of axial ligand. The concentration of the supporting electrolyte (tetraethylammonium perchlorate, TEAP) was ∼100 mM. Experiments were performed at 25 °C (scan rate 100 mV/s). All half-wave potentials were referenced internally with respect to the ferrocenium/ferrocene couple and expressed with respect to the saturated calomel electrode (SCE) considering the Fc^+/Fc couple to be +0.465 V vs SCE. Potentials were not corrected for the junction contribution. The nature of the couples (oxidation or reduction of the parent complex) was determined by measuring the rest potentials of the solutions. Electronic spectra were recorded in dichloromethane on a modified Cary 14 spectrophotometer with an OLIS interface and software. The cuvette compartment was attached to a circulating propylene glycol constant-temperature bath of 25.0 (±0.5) °C. NMR samples were prepared in CD_2Cl_2 (99.6%, Aldrich) in screw cap NMR tubes (Wilmad) and thoroughly degassed with argon; the spectra were recorded on a Varian Unity 300 MHz spectrometer. Data were processed on Sun Sparc Stations. All samples were frequency-locked with solvent deuterium and referenced to the residual solvent proton signal. The one-dimensional spectra were collected with a typical spectral width of about 30 kHz and 16K−32K data points; a 90° pulse width was used with a relaxation delay of 0.25 s; typically 512 transients were collected. Data were processed with 5−20 Hz exponential apodization before Fourier transformation.

X-Band electron paramagnetic resonance spectra (EPR) were collected on a Bruker ESP 300E spectrometer operating at ∼9.4 GHz. Samples were prepared as 0.5−2 mM solutions in a toluene and/or 2,5-dimethyltetrahydrofuran glass. Measurements at 77 K were made with a quartz liquid-nitrogen-immersion Dewar flask. Liquid-He measurements were made using an Oxford He cryostat.

Preparation of Compounds. All high-spin Fe(III) porphyrinates were synthesized as reported previously.[3,20] The corresponding low-spin complexes were generated from the high-spin complex in solution by addition of the desired imidazole bases.

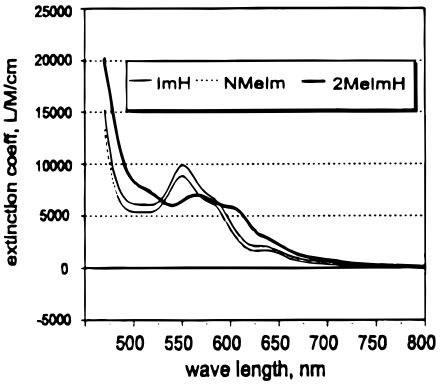

Figure 3. Electronic spectra of Fe(2,3-Mo-TTP)(B′)$_2$Cl (where B′ = ImH, NMeIm, 2MeImH). Perpendicular orientation of the axial ligand planes (2MeImH) shows a red shift from the parallel orientation (NMeIm and ImH).

Molecular Modeling. Molecular modeling simulations were performed on a Silicon Graphics IRIS system using the program SYBYL from Tripos Associates, Inc. The lowest energy van der Waals configurations were determined interactively using the MAXMIN2 energy minimization routine of SYBYL. The coordinates of LMoO and TTP were obtained from the Cambridge Structural Database. These fragments were then linked through a *meso* position with appropriate alterations, and the energy of the structure so obtained was minimized.

Measurement of Equilibrium Constants. Equilibrium constants were measured from the absorbances of ∼5.5 × 10^{-5} M dichloromethane solutions in a 1 cm path length cuvette according to the methods described earlier.[3] All measurements were made at 25 °C.

Results and Discussion

Syntheses and Spectra. The low-spin complexes [Fe(2,3-Mo-TTP)(2MeImH)$_2$]$^+$Cl$^-$ (**1**) and [Fe(3,4-Mo-TTP)(2MeImH)$_2$]$^+$Cl$^-$ (**2**) were generated in solution by adding a large excess of 2MeImH to a solution of the respective high-spin complexes, in an appropriate solvent (dichloromethane, dimethylformide). The color of the solution changed from brown to greenish brown, which is quite different from the red color of the bis-(*N*-methylimidazole) adduct. This difference is readily revealed in the electronic spectra (Figure 3). In the case of NMeIm as the axial ligand, the α and β bands appear around 550 and 580 nm; however, for 2MeImH they showed a red shift (bathochromic shift) of about 18 nm with smaller oscillator strength. This clearly indicates either that these two axial ligands have very different ligand field strengths or that the bands are strongly affected by the relative orientation of the axial ligands. We have also measured the equilibrium binding constants (β_2) for the formation of the bisadduct with the axial ligand 2MeImH in dichloromethane. The values are 1.82 (±0.6) × 10^3 and 2.29 (±2) × 10^3 M^{-2}, respectively, for **1** and **2**. The comparative values for [Fe(2,3-Mo-TTP)(NMeIm)$_2$]$^+$Cl$^-$ (**3**) and [Fe(3,4-Mo-TTP)(NMeIm)$_2$]$^+$ Cl$^-$ (**4**) are 7.54 (±0.8) × 10^4 and 3.94 (±0.2) × 10^4 M^{-2}, respectively.[3] The lower binding constants for **1** and **2** compared to those for **3** and **4** indicate that the formation of the 2MeImH adducts is less favorable than that of the NMeIm adducts. These results contrast with those for (tetraphenylporphinato)iron(III) complexes where NMeIm and 2MeImH show very similar binding constants.[21] Thus, the difference in the behavior of **1**−**4** must be due to the effects of the pendant molybdenyl fragment. It is well-known that

(19) Raitsimring, A. M.; Basu, P.; Shokhirev, N. V.; Enemark, J. H. *Appl. Magn. Reson.* **1995**, *9*, 173−192.

(20) LaBarre, M. J.; Raitsimring, A. M.; Enemark, J. H. In *Molybdenum Enzymes, Cofactors and Model Systems*; Stiefel, E. I., Coucouvanis, D., Newton, W. E., Eds.; ACS Symposium Series 535; Amerian Chemical Society: Washington, DC, 1993; pp 130−142.

electronic effects around the porphyrin periphery can be transmitted to the core nitrogen atoms and that the electronic contribution of the substituents can affect the axial ligand binding constants. We showed previously that the electronic effect of the molybdenyl fragment is very small.[9] Therefore, we believe that the difference (a factor of ∼50 for **1** and **3** and a factor of ∼20 for **2** and **4**) in the magnitude of the binding constants is not electronic but steric in origin, with the steric factor more important for **1**.

^{1}H NMR Spectra. For NMR measurements, samples were prepared in CD_2Cl_2. NMR spectra were recorded for both **1** and **2** in the temperature range +30 to −80 °C. We have been particularly interested in the pyrrole proton resonances that are sensitive reporters of unpaired electron spin delocalization in paramagnetic iron porphyrins.[1] We observed previously that $[Fe(2,3\text{-Mo-TTP})(NMeIm)_2]^+Cl^-$ (**3**) shows eight distinct pyrrole peaks that do not coalesce over the entire temperature range studied.[9] The majority of these peaks were shown unambiguously to arise from a single molecule by observation of spin connectivities resulting from either scalar or dipolar coupling. This led to the conclusion that at least *one axial NMeIm ligand is prevented from rotation, even at room temperature*. This finding, together with spin density calculations, allowed us to assign the preferred π-orbital for unpaired electron spin delocalization. From the mapping of the unpaired electron density, we concluded that the axial ligand whose rotation is "frozen" is aligned close to the *meso*-carbon carrying the bulky Mo(V) substituent and its opposite *meso*-carbon partner. Molecular modeling data supported the fact that the axial ligand on the same side of the porphyrinate plane as the molybdenum center can be prevented from rotation because of the steric bulk created by the tris(3,5-dimethylpyrazolyl)borate fragment. Moreover, from the large spread of the pyrrole resonances, we concluded that the other axial ligand (anti to the molybdenum center) either is rotating rapidly (on the NMR time scale) or is aligned parallel to the nonrotating ligand, but definitely not aligned perpendicular to it. Since 2MeImH has been shown to prefer perpendicular alignment of axial ligands in low-spin complexes, we expected that, if the rotation of one axial ligand can be stopped, then the other axial ligand should align itself in a mutually perpendicular fashion. In order to establish the relative orientation of the 2MeImH ligands, we have obtained NMR spectra for **1** and **2** in the temperature range +30 to −80 °C. Representative spectra for **1**−**4** are shown in Figure 4. For both compounds **1** and **2** we observed a very broad peak centered near −20 ppm at −60 °C. For **1** this broad peak can be assigned to a combination of at least four broad unresolved peaks. This clearly indicates that the separation of the energy of the orbitals (ΔE) is very small. This would be the case for mutually perpendicular axial ligand planes (Figure 1). Since the ligands in the perpendicular planes interact with two different d_π orbitals, the energies of both orbitals will be raised similarly and therefore lead to a small energy difference (ΔE_π). As a consequence, all of the pyrrole positions will have similar amounts of unpaired electron spin density, which is manifested by a small spread of the pyrrole peaks. In this case, we observe a very broad, nearly featureless peak. For the isomeric $[Fe(3,4\text{-Mo-TTP})(NMeIm)_2]^+Cl^-$ (**4**) we observed only three closely spaced resolved peaks centered near −27 ppm at −60 °C (Figure 4).[9] This clearly demonstrates that in **4** the tris(3,5-dimethylpyrazolyl)borate fragment is sufficiently far from the iron binding site so that the axial ligands are not prevented from rotation. This observation is in accord with our molecular modeling calculations. Therefore, we concluded that the small splitting of the pyrrole resonances in **4** is due to the unsymmetrical substitution of the porphyrinato ring and is not due to the axial ligand plane orientation. Since **2** has identical substituents on the porphyrinato ring, the same pattern of the pyrrole peaks would be expected if the substituent effect is the dominating factor. However, the observation of a single broad featureless peak for **2** indicates that the ligand planes are oriented perpendicularly and that the effect of ligand plane orientation is more important in determining the pyrrole proton shifts than is unsymmetrical substitution. From the variable-temperature NMR spectra of **1** and **2**, we can conclude that the effect of mutual ligand plane orientation predominates over the effect of hindered rotation of the axial ligand planes in unpaired electron spin delocalization.

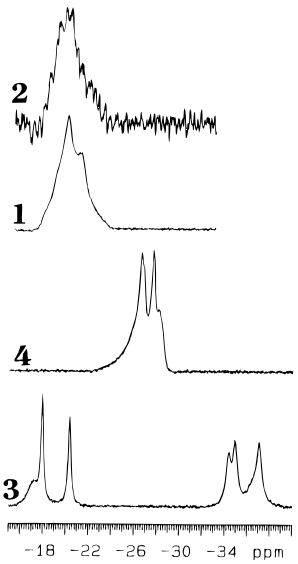

Figure 4. 300 MHz ^{1}H NMR spectra of the pyrrole protons at −60 °C in CD_2Cl_2, which clearly show the effect of orientation and hindered rotation of axial ligands on unpaired spin delocalization. From top to bottom: $Fe(3,4\text{-Mo-TTP})(2MeImH)_2Cl$ (**2**), $Fe(2,3\text{-Mo-TTP})(2MeImH)_2Cl$ (**1**), $Fe(3,4\text{-Mo-TTP})(NMeIm)_2Cl$ (**4**), and $Fe(2,3\text{-Mo-TTP})(NMeIm)_2Cl$ (**3**).

Electrochemistry. Both **1** and **2** were generated in DMF solution, and their redox behaviors were examined by cyclic voltammetry. Representative voltammograms are shown in Figure 5, and half-wave potentials are listed in Table 1. Both compounds exhibit pseudo-Nerstian one-electron reduction couples as evidenced by $i_{pa}/i_{pc} \sim 1$. Three distinct couples were observed in the negative part of the solvent window.

We will start the discussion with the most positive couple, which is due to the Fe(III/II) reduction. Changing the ligand plane orientation should change the energies of the orbitals to which the electron is to be added upon reduction of iron(III) to iron(II). Such a change in orbital energies would likely change the relative stabilities of the bis(ligand) complexes of the iron porphyrinates in the two oxidation states, which in turn would shift the redox potentials of the bis(ligand) complexes.[22] Thus, we expected a change in the redox potential if, at the time of electron transfer, the alignment of the ligand planes was different for the two types of axial ligands, as is expected for the $(NMeIm)_2$ and $(2MeImH)_2$ complexes of the iron(III) porphyrinates.[8] For the 3,4-Mo isomers (**2** and **4**), the potential of this couple is not significantly affected by changing the axial ligands from NMeIm to 2MeImH (Table 1). Similar Fe(III/II) reduction potentials are to be expected for isomers **2** and **4,**

(21) Walker, F. A.; Lo, M.-W.; Ree, M. T. *J. Am. Chem. Soc.* **1976**, *98*, 5552−5560.

(22) Nesset, M. J. M.; Shokhirev, N. V.; Enemark, P. D.; Jacobson, S. E.; Walker, F. A. *Inorg. Chem.* **1996**, *35*, 5188−5200.

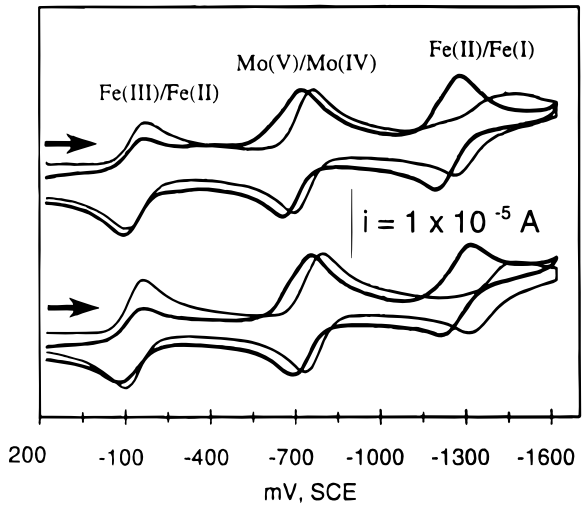

Figure 5. Cyclic voltammogams of **1**−**4** in DMF solution (1 mM) at 25 °C. Conditions: scan rate, 100 mV s^{-1}; supporting electrolyte, TEAP (0.1 M); potential expressed with respect to SCE; axial ligand concentration, ∼0.1 M. Top: **2** (bold line); **4** (light line). Bottom: **1** (bold line); **3** (light line). In each case, three distinct one-electron couples are observed.

Table 1. Electrochemical Data Obtained in DMF at 25 °C[a]

	$E_{1/2}$,[b] mV (ΔE_p,[c] mV)		
compd	$Fe^{III/II}$	$Mo^{V/IV}$	$Fe^{II/I}$
1	−156 (76)	−725 (63)	−1276 (104)
2	−135 (74)	−696 (73)	−1242 (81)
3[d]	−136 (62)	−764 (67)	−1473
4[d]	−142 (57)	−730 (63)	−1459

[a] Conditions: υ = 100 mV/s; supporting electrolyte, 0.1 M TEAP; working electrode, glassy carbon; potential referenced to SCE, calibrated against ferrocene (+0.465 V vs SCE) but uncorrected for junction contribution. [b] $E_{1/2} = 0.5(E_{pa} + E_{pc})$, where E_{pa} and E_{pc} are anodic and cathodic potentials, respectively. [c] $\Delta E_p = E_{pc} - E_{pa}$. [d] Taken from ref 3.

where the ligands are freely rotating, but not for the 2,3-Mo isomers (**1** and **3**), where at least one axial ligand is fixed. For the latter complexes, we observed a ∼20 mV negative shift in the redox potentials, indicating that the ratio $\log(\beta_2^{III}/\beta_2^{II})$ or $\log(\beta_2^{III}/K_1^{II})$ for **1** is larger than that for **3**. This indicates that the equilibrium constant for ligand binding suffers a larger decrease in size for **1** as compared to **3** than does **2** as compared to **4**. However, with the information available (Table 1) we cannot say whether the equilibrium constant is K_1^{II} or β_2^{II}. On the basis of a recent electrochemical study of equilibrium constants for binding pyridines and imidazoles to 2,6-phenyl-substituted (TPP)Fe^{III} derivatives,[22] we suspect that the Fe(II) complex binds only one 2-MeImH ligand at the concentrations used in this study. Thus, ligand loss probably accompanies reduction of **1** and **2** but not **3** and **4**. The rate constant for rotation of axial ligands (2MeImH) in a (tetramesitylporphyrinato)iron(III) complex at 25 °C measured by EXSY techniques is about 9.7×10^3 s^{-1} in dichloromethane.[23] At that temperature, there is also considerable ligand exchange between the free and bound ligands.[24] Thus, it is not possible to define the orientation of the axial ligands at the moment of electron transfer. It should also be noted that the N(1)−H hydrogen present in 2MeImH is capable of hydrogen bonding, which can also affect the potential. The difference in the potentials in **1** and **3** could also be due to the difference in the pK_a values[25] of NMeIm (7.33) and 2MeImH (7.56) (corrected for the presence of $2H^+$ (log 2)). The stronger the σ-donor strength of the axial ligand, the poorer the acid dissociation and the higher the pK_a. The higher the pK_a, the lower the reduction potential.

The middle peak in Figure 5 is due to the reduction of the molybdenum center from Mo(V) to Mo(IV). We noted earlier[3] that the (pyrazolylborato)oxomolybdenum center is a sensitive reporter of the porphyrin core structure. The Mo(V/IV) couple is cathodically shifted from the corresponding precursor complex,[3] where the porphyrin core is not metalated, because the iron(III/II) couple precedes it. When 2MeImH is used in place of NMeIm, the Mo(V/IV) couples for both the pairs **(1**, **3** and **2, 4)** shift anodically about 35−40 mV, making the reduction easier. Interestingly, the Mo(V/IV) couples of **1** and **2** (−725 and −696 mV, respectively) are more positive than that of the mononuclear precursor, LMoO(catechol) (−734 mV). This may simply indicate the difference in the electronic effect of 2MeImH and NMeIm. Formation of H-bonds between the coordinated 2MeImH and another ligand or solvent molecules can make the porphyrin center more electron rich, which should make it more difficult to reduce Mo(V) to Mo(IV). Alternatively, H-bond donation from noncoordinated 2MeImH to the catecholato oxygen atoms should favor the reduction of the molybdenyl center, as observed. The fact that **1** and **2** show such similar shifts in potential in the presence of 2MeImH further points to an effect of the excess ligand on the oxomolybdenum center. Therefore, the observed changes in the potential can be explained in terms of acid/base effects without invoking the distortion of the porphyrin core by the more bulky 2MeImH ligand. Thus, the electrochemistry shows that both metal centers behave primarily as independent redox centers with only small perturbations from the potentials of the individual isolated components.

The most significant differences in the potentials were observed for the Fe^{II}/Fe^{I} couple (see Table 1). However, since the Fe^{II}/Fe^{I} couple is extremely sensitive to axial ligand concentration (because β_2^{II} for Fe(II) is very large compared to β_1^{I} (or β_2^{I}) for Fe(I)[22] and their ratio is probably controlled by a number of factors), the shifts in potential are probably most directly related to the ratio of the binding constants, β_2^{II}/β_1^{I} and are thus not very relevant for the present work, which mainly focuses on the Fe(III) and Fe(II) oxidation states.

From Table 1 it can be seen that all the peaks for compound **1** are cathodically shifted by 20−40 mV relative to the corresponding peaks of **2**. This is presumably due to the fact that the two metal centers of **1** are closer together than those of **2**, and therefore there is more communication between the two centers in **1** than in **2**. This communication is probed in detail by EPR spectroscopy (*vide infra*).

EPR Spectra. Oxomolybdenum(V) ($S = {}^1/_2$) centers have long electronic relaxation times that make them extremely suitable for EPR studies. The isotropic X-band solution EPR spectra of nonmetalated porphyrins with a pendant molybdenyl fragment have $\langle g \rangle$ and $\langle A \rangle$ values very similar to those for the LMoO(catechol) complexes.[26] At 77 K these molecules display nearly axial spectra due to the pseudo-3-fold axis imposed by the three nitrogen atoms (of the facially coordinated tris(3,5-dimethylpyrazolyl)borate ligand, L) and three oxygen atoms (one oxo oxygen and two from the catechol fragment). Insertion of a diamagnetic metal into the porphyrin core does not change the Mo(V) EPR spectrum.[19] However, when a paramagnetic

(23) Shokhirev, N. V.; Shokhireva, T. K.; Polam, J. R.; Watson, C. T.; Raffii, K.; Simonis, U.; Walker, F. A. *J. Phys. Chem.* **1997**, *101*, in press.
(24) Nakamura, M. *Inorg. Chim. Acta* **1989**, *161*, 73−80.
(25) Albert, A. In *Physical Methods in Heterocyclic Chemistry*; Katritzky, A. R., Ed.; Academic Press: New York, 1971; Vol. I, pp 1−108.
(26) Basu, P.; Bruck, M. A.; Li, Z.; Dhawan, I. K.; Enemark, J. H. *Inorg. Chem.* **1995**, *34*, 405−407.

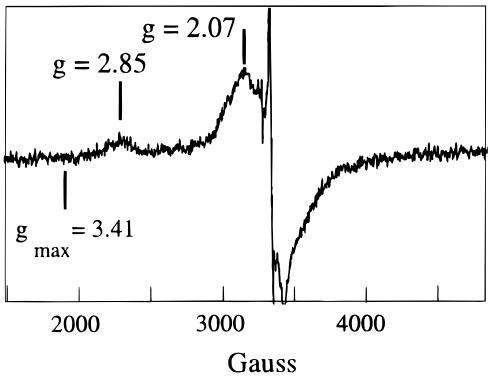

Figure 6. X-Band EPR spectrum of Fe(2,3-Mo-TTP)(2MeImH)$_2$Cl (**1**) at 4.2 K. The narrow signal is due a minor Mo(V) impurity. The large g_{max} signal occurs at 2.85 and is extremely low in amplitude compared to the Mo(V) signal. The position of the large g_{max} (3.41) of Fe(TTP)(2MeImH)$_2$Cl is shown for reference.

metal ion is inserted into the porphyrin core, the Mo(V) EPR spectra change dramatically. Insertion of high-spin iron(III) ($S = {}^5/_2$) reduced the intensity of the EPR signal, and the reduction of intensity could be correlated with the intermetal distance.[20] Addition of ligands (e.g., NMeIm) to the high-spin chloroiron complex generates the low-spin complex in which the energy separation between the two porphyrin valence π-orbitals (ΔE_π) is large. From a detailed EPR investigation at multiple frequencies and simulation of the respective spectra, we concluded that, for **4**, where the metal centers are separated by ~9.4 Å (as determined by computer modeling), the primary interaction is dipolar in nature. The observed spectra could be simulated by considering the intermetal interaction to be primarily dipolar in nature and allowing minor changes in the spectroscopic g values for the molybdenum center.[19] The g values for the molybdenum center in the simulated spectrum of **1** were 1.968, 1.943, and 1.939 (compared to 1.970, 1.968, and 1.925 for LMoO(catechol)). For **3**, however, the primary interaction is exchange, and the overall features of the spectrum of **3** were simulated by considering a distribution of exchange interactions.[3,19]

Changing the axial ligand from NMeIm to 2MeImH alters the interaction between the metal dπ orbitals of Fe(III) and the axial ligand nitrogen pπ orbitals. In contrast to the regular rhombic signal observed for NMeIm adducts of tetraphenylporphyrinates, 2MeImH adducts show a broad unresolved signal near $g \sim 3.4$, called "large g_{max}", and a very broad unresolved feature at higher field.[2,27] Another interesting feature of 2MeImH complexes is that their EPR spectra can only be observed at temperatures lower than 20 K, indicating a change in the relaxation parameters as well.[27]

In order to understand the effect of the axial ligand plane orientation on the spin−spin coupling, we have recorded the EPR spectra of **1** and **2** at liquid-helium temperature. We will discuss the case of complex **1** first. For **1** we observe (Figure 6) a shift of the g value of the iron center from the large g_{max} value of 3.41 to 2.85, a shift toward the g value of the molybdenum center, with an observed line width of ~200 G. The $g \sim 2$ region for **1** appears much cleaner than that for **3** because the central g value for the iron center in **3** (2.29) is absent.[3] However, the anisotropic nature of the molybdenum center is also lost. Only a broad signal (g =2.07, Figure 6) could be detected, and the molybdenum hyperfine structure is not resolved. This broad line is shifted toward lower field from its mononuclear precursor complex. From molecular modeling calculations, we found that the two metal centers are separated by ~7.9 Å in both **1** and **3**. This distance gives a characteristic value for the dipolar interaction of $g\beta r^{-3} \sim 40$ G (0.004 cm^{-1}) at the iron center, which is much lower than the observed line width. This estimate is much smaller than the exchange integral estimated below, indicating that the spin−spin interaction is dominated by exchange. For **3**, g_1 of the iron center was moved from 2.92 (for Fe(TTP)(NMeIm)$_2$Cl) to 2.70.[19] From the shift in the g values, we can estimate the amount of exchange interaction (J) according to the relation $J \approx \nu\ (\delta g/g_e)$, where δg is the change in the g value due to exchange, ν is the microwave frequency, and g_e is the g value of the free electron. This gives rise to an exchange interaction of ~1 GHz (0.03 cm^{-1}) for **3**. For **1**, the large g_{max} changes from 3.41 (for Fe(TTP)(2MeImH)$_2$Cl) to 2.85, which gives rise to an estimated J of 2.6 GHz (0.078 cm^{-1}). Qualitatively, this difference in the exchange interaction can be explained by invoking the fact that the nonplanarity of the porphyrin ring caused by the steric bulk of 2MeImH may allow stronger interaction between the two metal centers in **1**, thereby increasing the exchange interaction.

It should be noted that a single exchange integral alone cannot explain the complete disappearance of the anisotropic feature of the molybdenum center as observed in the EPR spectra of **1** and **3**. For compound **3**, we explained the general features of the molybdenum signal by considering a distribution of exchange integrals.[3] Such a distribution is possible if at least one axial ligand is freely rotating in fluid solution and can adopt a range of orientations in frozen solution. Furthermore, from our detailed investigations of compound **3** utilizing NMR spectroscopy, we concluded that although one axial ligand (syn to the molybdenum center) is prevented from rotation, the other axial ligand can rotate freely or adopt an orientation parallel to the hindered one. Furthermore, the hindered axial ligand is not completely static and shows some mobility in solution.[9] Thus, the dynamics of the axial ligands can allow several slightly different rotational isomers in solution. These conformational variations can lead to a distribution of exchange integrals in **3** measured in a frozen solution.[3] From the solution NMR investigation of compound **1** (*vide supra)*, we know that the two axial ligands are in perpendicular orientation and one ligand (syn to the molybdenum center) is prevented from rotation. This implies that the second axial ligand (anti to the molybdenum center) is also prevented from rotation. However, we believe that the ligands are not completely static in compound **1** and show several slightly different rotamers in solution. These rotamers again can give rise to a distribution of exchange integrals. Thus, for **1** the primary interaction is exchange and a distribution of rotamers will give a distribution of exchange integrals.

The molybdenum part of the spectrum of **2** shows spectral features almost identical to those of **4**. It thus appears that the coupling in **2** is also primarily dipolar in nature, with the g values of the molybdenum center slightly changed from those of the precursor complex, as observed for **4**.[19] It is well-known that the dipolar interaction depends on the interspin distance. Changing the axial ligands from NMeIm to 2MeImH does not significantly alter the intermetal distance (~9.4 Å), and thus, the dipolar interaction is not expected to change, assuming the relative orientations of the **g** tensors are the same. The EPR spectra arising from the low-spin iron(III) centers of **2** and **4** are distinctly different; **2** shows a large g_{max} signal of 3.4 and a larger observable line width than **4**, which has a rhombic spectrum with $\langle g \rangle$ of 2.25. The upper limit for dipolar

(27) Walker, F. A.; Reis, D.; Balke, V. L. *J. Am. Chem. Soc.* **1984**, *106*, 6888−6898.

interaction for **2** calculated from the empirical relation ($\approx g\beta r^{-3}$) is 50 G, which is smaller than the observed line width for the iron(III) centers ($\sim$150 G) at this frequency. This large line width obscures any dipolar splitting of the Fe(III) signal of **2**.

Summary. The proton NMR spectra of **1**, the bis(2-methylimidazole) adduct of Fe(2,3-Mo-TTP)Cl, are characteristic of perpendicular ligand plane orientation. In contrast, **3**, the bis(*N*-methylimidazole) adduct, shows a large spread of the pyrrole resonances that is indicative of nonperpendicular axial ligand plane orientation. For **2,** the bis(2-methylimidazole) adduct of Fe(3,4-Mo-TTP)Cl, the ligands are found to be in perpendicular orientation, whereas **4**, the bis(*N*-methylimidazole) adduct, has the ligands oriented in parallel planes. To the best of our knowledge, **1**−**4** are the first complexes to show the dramatic effects of ligand plane orientation, even at room temperature. Compounds **1** and **2** have smaller binding constants than those of **3** and **4**, indicative of differences in the steric demands of the axial ligands. The reduction potentials of the Mo(V/IV) couple act as a sensitive reporter of the porphyrin core events, and the cathodic shifts of the couples of the 2,3-isomers relative to those of the 3,4-isomers indicate that communication between the two metal centers increases as the distance between the two metal centers decreases. We also observe a difference in the reduction potential of the Fe(III/II) couple between **1** and **3** that may be due to the axial ligand orientation effect. However, more experiments are needed in order to test this hypothesis. The overall EPR spectra of the Mo(V) region of **1**−**4** are independent of the nature of the axial ligand (NMeIm vs 2MeImH), in spite of the fact that the EPR spectra of the isolated low-spin Fe(III) porphyrinate centers are dramatically different from one another. This indicates that the nature of the spin−spin coupling between the molybdenum center and the heme center in these molecules is not substantially affected by ligand plane orientation even though the magnitudes of the exchange interactions are quite different for **1** and **3**. This observation may have implications for proteins in which the heme center is spin-coupled with one or more other paramagnetic centers, and suggests that the ligand plane orientation imposed by the heme pocket backbone may have little effect upon the spin−spin coupling pattern. Ongoing studies in our laboratories will further explore this hypothesis.

Compounds **1** and **3** constitute a class of molecules heretofore unknown in model heme chemistry in which rotation of axial ligands is stopped even at room temperature. From our detailed NMR investigation on **3**, we concluded that one axial ligand (syn to the molybdenum center) was frozen by steric interactions. However, the data for **3** did not enable us to determine whether the second axial ligand (anti to the molybdenum center) was rotating rapidly or locked parallel to the first ligand.[9] The present study shows that the two axial ligands of **1** are in perpendicular orientation and that one axial ligand (syn to the molybdenum center) is prevented from rotation; this implies that the second ligand is also not rotating. These results for **1** lead to the provocative suggestion for compound **3** that the anti axial ligand adopts a locked parallel conformation. Finally, we note that the attachment of a bulky group at the periphery of the porphyrin macrocycle is a good strategy for mimicking the rigidity of the axial ligand binding in heme pockets.

Acknowledgment. We thank Jeff L. Weibrecht and Julie Graff for experimental assistance and Andrew B. Uplinger for aid in drawing Figure 1. Support of this research by the National Institutes of Health (Grant GM-37773 to J.H.E. and Grant DK-31038 to F.A.W.) and the Materials Characterization Program of the University of Arizona is gratefully acknowledged. We also thank the National Science Foundation for funds to purchase the EPR (Grant DIR-9016385) and NMR (Grant CHE-9214383) spectrometers.

IC960945A